the plant journal

SEB Society for Experimental Biology

The Plant Journal (2012) **70**, 243–255 doi: 10.1111/j.1365-313X.2011.04861.x

Unraveling the regulatory network of the MADS box transcription factor RIN in fruit ripening

Guozheng Qin[1,*,†], Yuying Wang[1,2,†], Baohua Cao[1,2], Weihao Wang[1,2] and Shiping Tian[1,2,*]

[1]*Key Laboratory of Plant Resources, Institute of Botany, Chinese Academy of Sciences, No. 20 Nanxincun, Xiangshan, Haidian District, Beijing 100093, China, and*

[2]*The Graduate University of the Chinese Academy of Sciences, Yuquanlu, Beijing 100049, China*

Received 8 October 2011; accepted 17 November 2011; published online 19 December 2011.

*For correspondence (fax +86 10 62836463; e-mail gzqin@ibcas.ac.cn or fax +86 10 82594675; e-mail tsp@ibcas.ac.cn).

†These authors contributed equally to this work.

SUMMARY

The MADS box transcription factor RIN is a global regulator of fruit ripening. However, the direct targets modulated by RIN and the mechanisms underlying the transcriptional regulation remain largely unknown. Here we identified 41 protein spots representing 35 individual genes as potential targets of RIN by comparative proteomic analysis of a *rin* mutant in tomato fruits. Gene expression analysis showed that the mRNA level of 26 genes correlated well with the protein level. After examining the promoter regions of the candidate genes, a variable number of RIN binding sites were found. Five genes (*E8*, *TomloxC*, *PNAE*, *PGK* and *ADH2*) were identified as novel direct targets of RIN by chromatin immunoprecipitation. The results of a gel mobility shift assay confirmed the direct binding of RIN to the promoters of these genes. Of the direct target genes, *TomloxC* and *ADH2*, which encode lipoxygenase (LOX) and alcohol dehydrogenase, respectively, are critical for the production of characteristic tomato aromas derived from LOX pathway. Further study indicated that RIN also directly regulates the expression of *HPL*, which encodes hydroperoxide lyase, another rate-limiting enzyme in the LOX pathway. Loss of function of RIN causes de-regulation of the LOX pathway, leading to a specific defect in the generation of aroma compounds derived from this pathway. These results indicate that RIN modulates aroma formation by direct and rigorous regulation of expression of genes in the LOX pathway. Taken together, our findings suggest that the regulatory effect of RIN on fruit ripening is achieved by targeting specific molecular pathways.

Keywords: MADS-RIN, proteomics, chromatin immunoprecipitation, fruit ripening, transcription factor, tomato.

INTRODUCTION

Fruits are developmental structures that are unique to flowering plants and play a central role in seed maturation and dispersal. Fleshy fruits are enriched with nutrients, such as flavor compounds, fiber, vitamins and antioxidants, that make them an important component of human diets (Alba *et al.*, 2005). Fruit ripening is a complex, genetically programmed process that is characterized by dramatic changes in the color, texture, flavor and aroma of the fruit flesh (Giovannoni, 2004). Various internal and environmental factors, including developmental signals and genes, hormones, light and temperature, participate in this process (Matas *et al.*, 2009). Based on their different ripening mechanisms, fruits are classically divided into two groups: climacteric and non-climacteric (Lin *et al.*, 2009). Climacteric fruits (e.g. tomato, apple, banana, avocado) show a burst in respiration and a typical increase in biosynthesis of the gaseous hormone ethylene at the onset of ripening, whereas non-climacteric fruits (e.g. strawberry, grape, citrus) do not require climacteric respiration or increased ethylene for ripening (Alexander and Grierson, 2002). Ethylene has been studied extensively due to its crucial role in ripening of climacteric fruits (Oeller *et al.*, 1991; Hackett *et al.*, 2000; Barry and Giovannoni, 2006; Kevany *et al.*, 2007). A great deal is known regarding ethylene biosynthesis, ethylene perception and signal transduction, and downstream gene regulation in ripening of climacteric fruits (Lin *et al.*, 2009). However, understanding of the regulatory mechanism of ripening in non-climacteric fruits and the upstream regulation of ethylene in climacteric fruits remains elusive.

Recent advances in the study of fruit-specific transcriptional control of ripening in tomato (*Solanum lycopersicum*) have received considerable attention. The products of the *RIPENING-INHIBITOR* (*RIN*) and *TOMATO AGAMOUS-LIKE1* (*TAGL1*) MADS box gene (Vrebalov *et al.*, 2002, 2009; Ito *et al.*, 2008), the *COLOURLESS NON-RIPENING* (*CNR*) SPB box gene (Manning *et al.*, 2006), the *LeHB-1* homeobox gene (Lin *et al.*, 2008) and *APETALA2a* (*AP2a*) (Karlova *et al.*, 2011) have been shown to act upstream of ethylene regulation of ripening in tomato. The MADS box transcription factor RIN is especially interesting, as the *rin* mutation has been bred into many commercial tomato varieties to delay ripening and extend the shelf-life of the fruit (Giovannoni, 2007). The homozygous *rin* mutation effectively blocks the ripening process and results in green/yellow tomato fruits that do not produce elevated ethylene levels and do not ripen in response to exogenous ethylene (Vrebalov *et al.*, 2002). Moreover, the *RIN* gene appears to be conserved between climacteric and non-climacteric fruits, implying that RIN may represent a global developmental regulator of fruit ripening. Although the biochemical and physiological downstream effects of RIN on ripening have been well documented, little is known about the genes that are directly regulated by RIN. The regulatory role of RIN on fruit ripening is partly associated with its regulation of ethylene metabolism. It has been shown that RIN directly regulates the expression of two ethylene anabolic genes (*ACS2* and *ACS4*) by binding to CArG box elements, the typical binding sequence for MADS box proteins, in their promoters (Ito *et al.*, 2008; Fujisawa *et al.*, 2011). However, other molecular pathways that are directly regulated by RIN remain largely unknown. Such information is critical to elucidate the regulatory cascade controlled by RIN and to understand the connections with other regulatory networks controlling normal fruit ripening.

Proteomics has become a powerful tool that, when combined with complementary molecular, cellular and physiological techniques, provides a framework for understanding the molecular basis of complex biological processes (Cravatt *et al.*, 2007). Previous studies have shown that a proteomics-based approach is useful to obtain insight into the molecular pathways that are directly regulated by transcription factor in various organisms (Lelong *et al.*, 2007; Song *et al.*, 2008; Azkargorta *et al.*, 2010). Here we used high-resolution two-dimensional (2D) electrophoresis coupled with chromatin immunoprecipitation (ChIP) to identify RIN-regulated direct target genes for control of tomato fruit ripening. We found that RIN bound to the promoters and directly modulated the expression of five target genes. Furthermore, we provide evidence that RIN rigorously modulates generation of aroma compounds via the lipoxygenase (LOX) pathway. Our findings suggest that RIN regulates fruit ripening by targeting specific molecular pathways.

RESULTS

Proteomic identification of potential downstream targets of RIN

To identify the potential targets of RIN, we examined the differential proteome profiles between wild-type and *rin* mutant tomato fruits. The *rin* lesion results in deletion of the last exon of *RIN*, causing fusion of *RIN* to the coding sequence of the adjacent gene, and leads to the loss of function of the RIN protein (Giovannoni, 2004). All ripening phenomena were abolished in the *rin* mutant (Vrebalov *et al.*, 2002). Consistent with previous reports, we observed enlarged sepals and loss of inflorescence determinacy in *rin* plants. Additionally, the *rin* tomato fruit have an altered pericarp color and show delayed ripening processes (Figure 1a).

MADS box genes in plants have been shown to be expressed in tissue-specific patterns. Consistent with the data obtained by Ito *et al.* (2008), we found that expression of the *RIN* gene and protein occurred during fruit ripening in the wild-type fruit (Figure 1b), commencing at the mature green stage and continuing to the red ripe stage. In the *rin* mutant, an absence of *RIN* gene and protein expression was observed throughout the period of normal *RIN* expression.

Proteins from *rin* mutant and wild-type fruits were separated by 2D gel electrophoresis and the representative gel images are shown in Figure 1(c). The experiment was performed with at least three biological repeats, and the gel images were analyzed using Image Master 2D Elite software. Approximately 900 spots were detected on each 2D gel after ignoring very faint spots and spots with undefined shapes and areas. A total of 126 protein spots exhibited significant changes in abundance in the *rin* mutant compared with the wild-type fruit, as analyzed by Student's *t* test ($P < 0.05$). Of these protein spots, 47 showed more than twofold changes in abundance (Figure 1c). Each of these spots was excised from the gels and submitted to Q-TOF MS/MS analysis. Forty-one protein spots representing 35 individual genes were successfully identified by database searching with the Mascot search engine (Table S1). These proteins were classified into functional categories according to the FunCat annotation scheme (http://mips.gsf.de/proj/funcatDB) (Figure S1) (Ruepp *et al.*, 2004).

Effects of the *rin* mutation on the overall pattern of protein expression

The data for differentially expressed proteins were extracted from the proteome data, and grouped (clustered) to reveal patterns of protein expression. Proteins were clustered according to the changes in protein intensity between wild-type and the *rin* mutant using the unweighted pair group method with arithmetic mean (UPGMA) (Caraux and

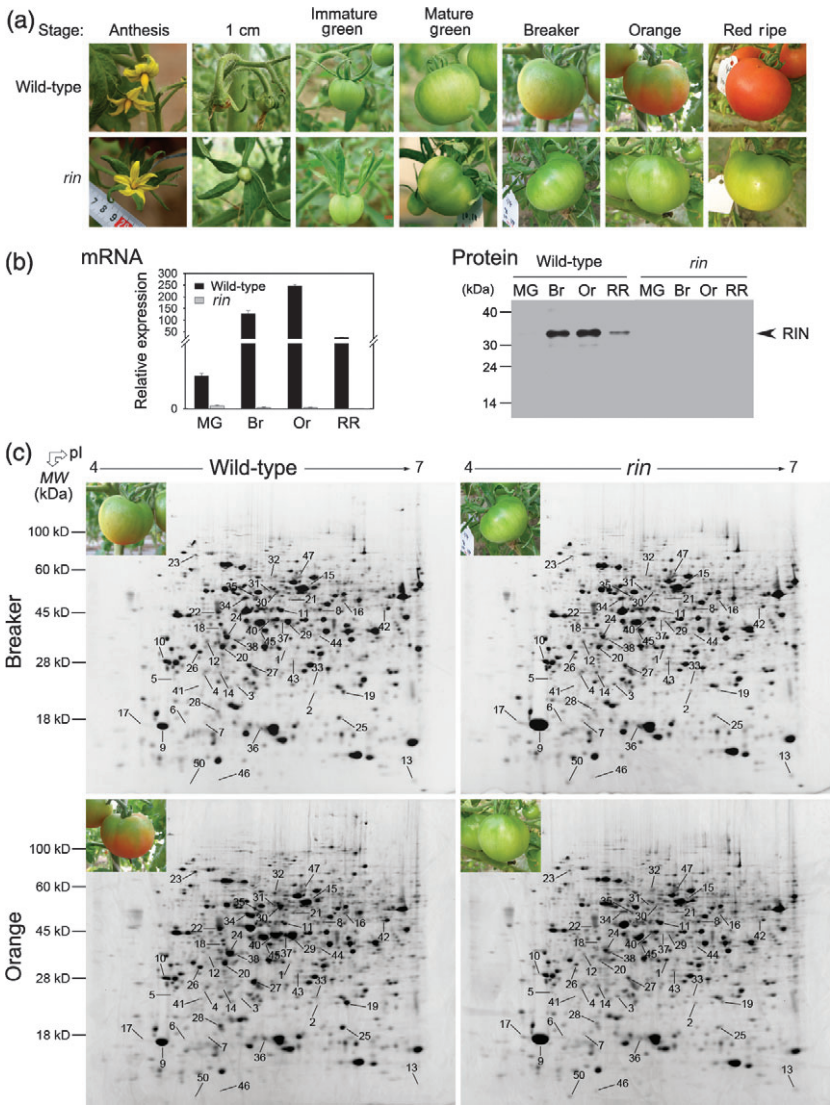

Figure 1. Changes in protein expression profile in *rin* mutant reveal the potential downstream targets of RIN.
(a) The phenotype of the *rin* mutant tomato. The *rin* lesion resulted in the enlargement of sepals and loss of inflorescence determinacy, altered pericarp color, and blocked fruit ripening. The stages of fruit ripening include immature green (IG), mature green (MG), breaker (Br), orange (Or) and red ripe (RR).
(b) Absence of RIN expression in the *rin* mutant during fruit ripening. The transcript levels were determined by quantitative RT-PCR, and the protein levels were examined by Western blotting. The *18S rRNA* gene was used as an internal control in the quantitative RT-PCR analysis. Values are means ± SD of three independent experiments.
(c) Proteomic identification of differentially expressed proteins between wild-type and *rin* mutant fruits at breaker and orange ripening stages. Proteins (500 μg) were separated on Immobiline Drystrip (GE Healthcare, http://www.gehealthcare.com) with a linear pH gradient from 4–7 in the first dimension and by SDS–PAGE in the second dimension, followed by visualization by Coomassie blue staining. Numbers indicate proteins that were differentially expressed in the mutant and subsequently identified by mass spectrometry (listed in Table S1).

Pinloche, 2005). We found three main clusters of proteins with differential expression patterns between wild-type and *rin* at the transition from breaker to orange ripening stage (Figure 2a). Cluster I (approximately 39.0% of all spots) comprised 16 proteins whose abundance was up-regulated in the *rin* mutant, particularly in fruit at the orange stage. Half of these proteins are associated with photosynthesis (Figure 2b). The abundance of these proteins generally decreased from breaker to orange stage in wild-type fruit, correlating with the differentiation of chloroplasts into chromoplasts. Cluster I also included three proteins with functions related to amino acid metabolism and five proteins related to other biological functions. Clusters II and III comprised proteins whose abundance decreased in the *rin* mutant (Figure 2a). Cluster II (approximately 14.6% of all spots) comprised six proteins that showed high levels of expression in both breaker and orange wild-type fruits, but were down-regulated in *rin* fruits at these ripening stages. These proteins are involved in amino acid metabolism (spot 29), carbohydrate metabolism (spots 22 and 35), intracellular signaling (spots 10 and 26), and stress responses (spot 23) (Figure 2b). Cluster III (approximately 46.3% of all spots) comprised 19 proteins associated with diverse biological functions. The abundance of these proteins was down-regulated in *rin* fruits at the orange ripening stage.

Gene expression patterns correlated with protein expression patterns detected in proteomics analysis

To examine whether the protein expression patterns were also present at the transcript level, quantitative RT-PCR was performed using RNA samples from three independent collections of wild-type and *rin* mutant fruits at the orange ripening stage. All the genes encoding the proteins listed in Table S1 were used for quantitative RT-PCR analysis except

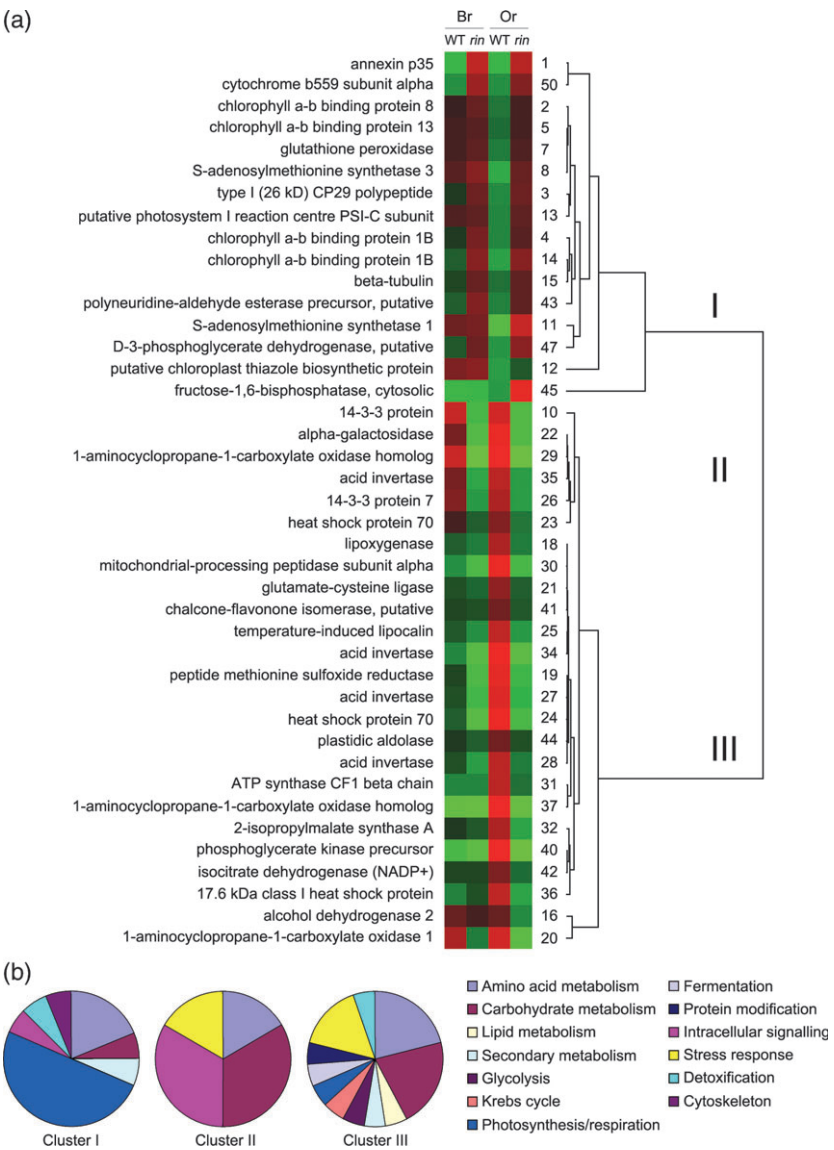

Figure 2. Hierarchical clustering analysis of the changes in protein expression between wild-type and *rin* fruit.
(a) Spots listed in Table S1 were clustered into three clusters (I, II and III) according to their percentage of volume using the Pearson clustering algorithm. Each row in the color heat map indicates a single protein, and each column represents proteins from wild-type (WT) and *rin* fruit at the breaker (Br) and orange (Or) ripening stages. A bright red color indicates a high protein expression value for a specific protein spot, and a bright green color represents a low protein expression value. For each protein, the spot number and the functional annotation are shown.
(b) Functional classification of proteins in each cluster.

those encoded by the chloroplast genome. The gene sequences were obtained from the Sol Genomics Network (SGN) tomato unigene database (http://solgenomics.net). Our results showed that, for 26 genes (approximately 81.3% of all genes detected), the transcript alterations were in agreement with the protein expression variations (Figure 3). However, differences in the magnitudes of changes were observed between the quantitative RT-PCR and proteome analysis. Several genes had much higher fold changes in quantitative RT-PCR, such as those encoding peptide methionine sulfoxide reductase (E4; spot 19) and acid invertase (TIV1; spot 27). Other genes showed different patterns of expression between mRNA and protein levels. These included genes encoding *S*-adenosylmethionine synthetase 1 (spot 11), *S*-adenosylmethionine synthetase 3 (spot 8) and α-galactosidase (spot 22).

RIN binds directly to the promoter regions of five genes *in vivo*

Expression data obtained from the proteome analysis and quantitative RT-PCR showed that RIN regulates genes with various biological functions. To identify the target genes that are directly regulated by RIN, a ChIP assay was performed. A previous report showed that RIN binds to the CArG box element [C(C/T)(A/T)(A/T)(A/T)(A/T)(A/T)(A/T)(A/G)G], which is the typical binding site for MADS box transcription factors (Ito *et al.*, 2008). We examined the the presence of CArG box elements in the 2000 bp upstream region starting from the translational start site (ATG) of those genes that were selected for quantitative RT-PCR analysis. The results indicated that the promoters of seven genes (approximately 21.9% of all genes detected)

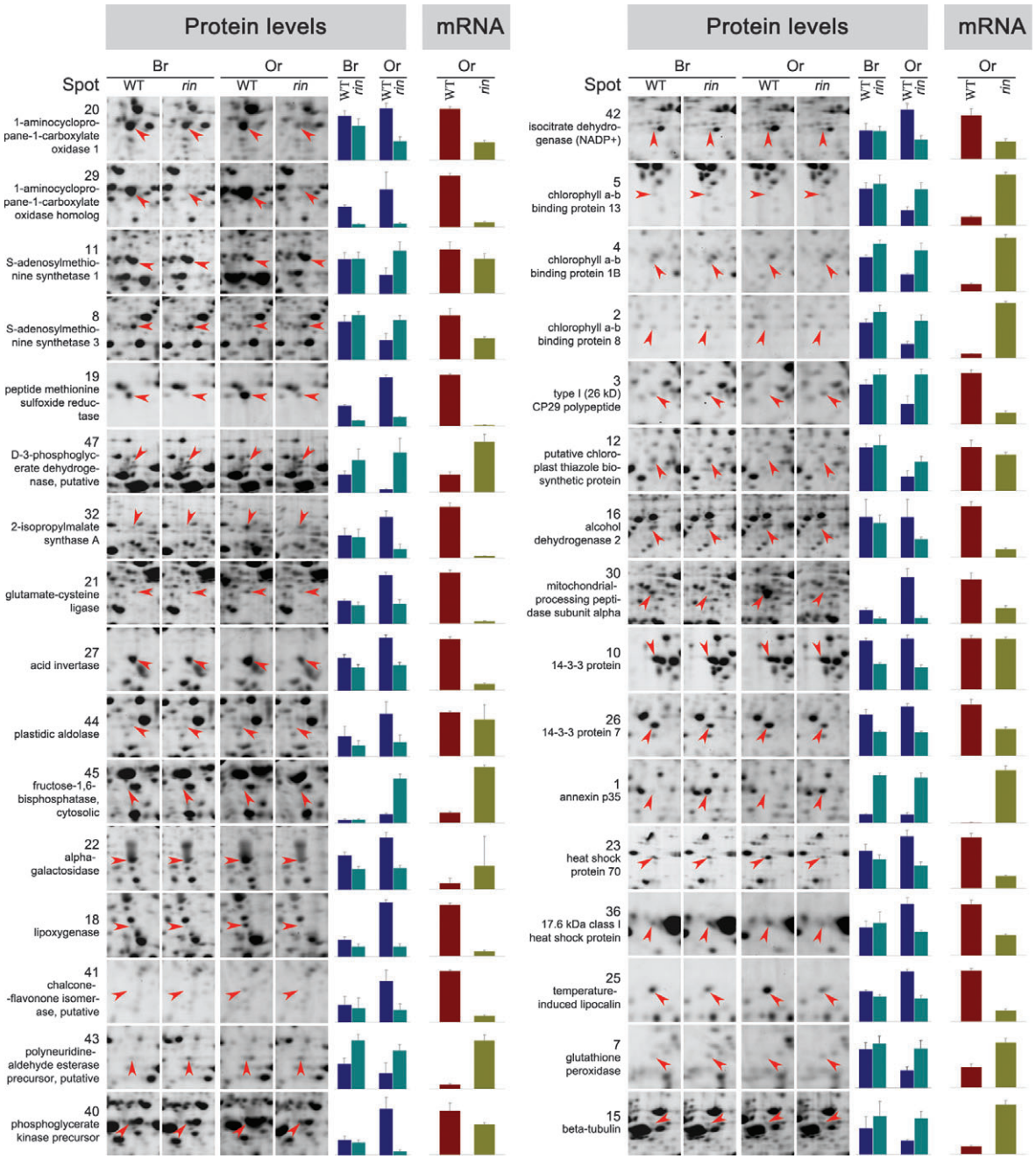

Figure 3. Comparison of gene expression profiles at protein and mRNA levels.
Differential protein expression between wild-type (WT) and the *rin* mutant was revealed by 2D gel electrophoresis at breaker (Br) and orange (Or) ripening stages. Histograms show the changes in protein abundance. The spot number on the 2D gels and the functional annotation for each protein are shown. The mRNA expression levels were measured by quantitative real-time PCR at the orange stage. The gene transcript levels are indicated as fold changes after normalization against the *18S rRNA* gene, followed by normalization against the wild-type. The results for protein and mRNA expression are means ± SD from three independent experiments.

contained four or more CArG box binding motifs, the promoters of eight genes (approximately 25.0% of all genes detected) contained three CArG box binding motifs and the promoters of eight genes (approximately 25.0% of all genes detected) contained two CArG box binding motifs (Table S2). Of the remaining genes, eight (approximately 25.0% of all genes detected) had only one motif in their promoter regions, and one did not contain a CArG box motif.

For the ChIP assay, cross-linked DNA–protein complexes were immunoprecipitated using affinity-purified anti-RIN

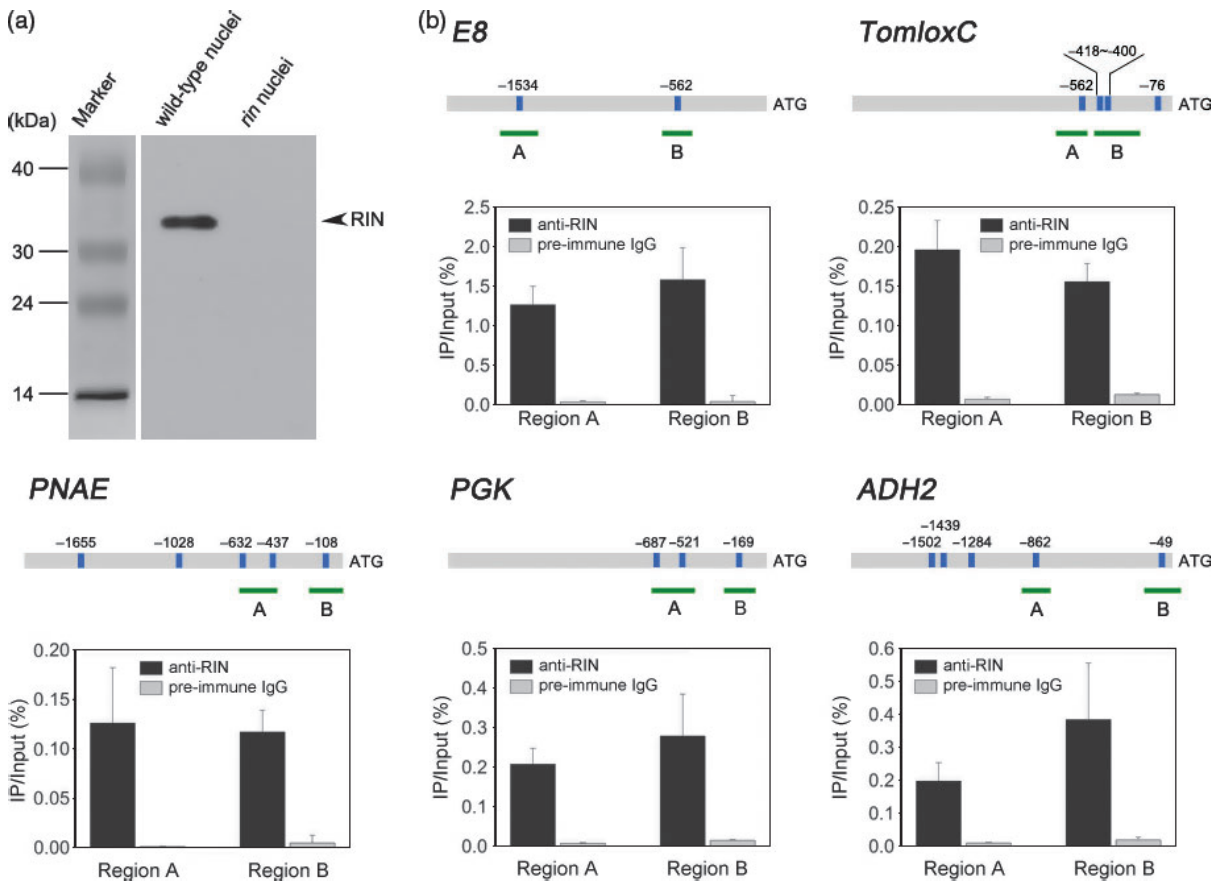

Figure 4. RIN directly binds to the promoters of five genes as revealed by chromatin immunoprecipitation.
(a) Western blot analysis of the specificity of the purified RIN polyclonal antibodies used for chromatin immunoprecipitation (ChIP) assay. Nuclear proteins from wild-type and the *rin* mutant fruit at the orange ripening stage were hybridized with affinity-purified RIN polyclonal antibodies.
(b) ChIP-qPCR shows the binding of RIN to the promoters of the regulatory targets. The promoter structures of the various target genes are shown. Blue boxes indicate CArG box elements; numbers indicate the position of these motifs relative to the translational start site; green fragments with upper-case letters indicate the regions used for ChIP-qPCR. Values are the percentage of DNA fragments that co-immunoprecipitated with anti-RIN antibodies or non-specific antibodies (pre-immune rabbit IgG) relative to the input DNA. Error bars represent the SD of three independent experiments.

polyclonal antibody. Protein gel-blot analysis verified that the purified RIN antibody reacts exclusively with the RIN protein (Figure 4a). Specific primers were designed to amplify promoter sequences surrounding CArG box binding sites from the immunoprecipitated DNA (Table S3). All the genes containing CArG box binding motifs in their promoters were detected. The binding of RIN protein to the promoter of *ACC synthase 2* (*ACS2*), a known RIN-target gene (Ito *et al.*, 2008), was used as a positive control.

Combination of ChIP with quantitative PCR (ChIP-qPCR) showed specific enrichment for the promoter regions of five genes of the 32 putative target genes tested when the affinity-purified RIN antibodies were used compared with when non-specific antibodies (pre-immune rabbit IgG) were used (Figure 4b). Some of the promoter fragments were precipitated to a much greater extent than others, suggesting that RIN has differential binding ability to the promoter fragments *in vivo*. Among these direct target genes, we paid particular attention to *TomloxC* and *ADH2*, which encode lipoxygenase (LOX) and alcohol dehydrogenase 2 (ADH2), respectively, because these two genes are involved in the same process, i.e. the LOX pathway, leading to formation of aroma volatiles.

In addition, the ChIP assay indicated that RIN binds directly to the promoter region of the *E8* gene (Figure 4b), which encodes a 1-aminocyclopropane-1-carboxylate oxidase homolog that is required for ethylene synthesis (Giovannoni, 2004). RIN was also shown to bind directly to the promoter of the *PNAE* gene (spot 43), which encodes polyneuridine aldehyde esterase, an enzyme that is involved in the biosynthesis of sarpagine-type alkaloids, and to that of the *PGK* gene (spot 40), which encodes phosphoglycerate kinase, a transferase used in the 7th step of glycolysis. Notably, except for *PNAE*, all of the RIN direct target genes were down-regulated in the *rin* mutant.

Gel mobility shift assay showing the *in vitro* binding ability of RIN

To confirm that RIN binds to the promoters of genes identified in the ChIP assay, we performed an electrophoretic mobility shift assay (EMSA) with purified recombinant RIN protein (Figure 5a). We produced double-stranded and biotin-labeled probes (26-mer oligonucleotide) containing the CArG box elements for each gene (*E8*, *TomloxC*, *PNAE*, *PGK* and *ADH2*), and studied their binding by the RIN protein. A shift band was observed for each gene when the RIN protein was mixed with the biotin-labeled probe (Figure 5b). Formation of the DNA–protein complexes was effectively competed by addition of an excessive amount of the corresponding unlabeled probe, especially at the highest competitor concentration. These results show that RIN binds specifically to the biotin-labeled probe. Different extents of competition by the unlabeled DNA fragment were observed, indicating that RIN has differential binding ability to the promoters of these genes.

RIN directly regulates gene expression in the LOX pathway during fruit ripening

The results of the ChIP assay and the EMSA have shown that RIN directly binds to the promoters of *TomloxC* and *ADH2*, which encode rate-limiting enzymes in the LOX pathway. We then investigated the dynamic changes in gene expression at the level of mRNA transcription to examine the direct regulation of *TomloxC* and *ADH2* by RIN. As shown in Figure 6(a), mRNA of *TomloxC* was detected at relatively low levels at the mature green stage of ripening, increasing at breaker stage, and remaining at high levels thereafter in wild-type fruits. In contrast, the expression of *TomloxC* was significantly inhibited in the *rin* mutant during fruit ripening. *ADH2* transcripts showed similar expression patterns as those observed for *TomloxC*. In the wild-type, the mRNA occurred at mature green stage, with increased transcript levels detected at the breaker and orange stage, and the levels then decreased. The expression of *ADH2* in the *rin* mutant was significantly reduced, persisting at low levels throughout the ripening process.

The expression of the *HPL* gene, which encodes hydroperoxide lyase, another rate-limiting enzyme in the LOX pathway, was also examined, although this enzyme was not identified in our proteomic analysis. Figure 6(a) shows that *HPL* expression increased during fruit ripening in wild-type fruit, peaking at the orange stage, and declined thereafter. *HPL* mRNA was also detectable during the period of fruit ripening in the *rin* mutant, but the mRNA levels were lower than detected in the wild-type. We then assessed whether RIN binds directly to the promoter region of *HPL*. Examination of the 2000 bp upstream region starting from ATG indicated that there are six CArG box elements in the promoter of *HPL*. Direct binding of RIN to the *HPL* promoter was observed in the ChIP-qPCR experiment, with much higher relative amounts of precipitated promoter fragments of *HPL* in experiments using anti-RIN antibodies than those using pre-immune rabbit IgG (Figure 6b). The binding ability of RIN to the promoter of *HPL* was further confirmed by EMSA (Figure 6c).

LOX-derived biosynthesis of volatile aroma compounds is regulated by RIN

Aroma volatiles in tomatoes and other fruits normally accumulate late during maturation (Lewinsohn *et al.*, 2001). As the RIN transcription factor directly regulated the expression of genes in the LOX pathway, we determined the contents of hexanal, *trans*-2-hexanal, hexenol and *cis*-3-hexanol, which are representative aroma products derived from LOX pathway, in the *rin* mutant and wild-type control at various ripening stages of tomato fruit. At the mature green stage, the levels of hexanal and *trans*-2-hexanal in wild-type fruits were negligible, but in later stages of development they reached 1690.8 and 139.6 $\mu g\ g^{-1}$ fresh weight, respectively (Figure 7a,b). By comparison, hexanal and *trans*-2-hexanal were produced at constitutively low levels throughout fruit ripening in the *rin* mutant fruit. The abundance of hexenol and *cis*-3-hexanol was also significantly reduced in the *rin* mutant (Figure 7c,d). The differences between wild-type and *rin* mutant for both hexenol and *cis*-3-hexanol were reduced at later stages of ripening.

DISCUSSION

RIN directly regulates LOX-derived generation of aroma compounds

The aroma is one of the most important quality attributes of tomato (Dirinck *et al.*, 1977). Over 400 aroma volatiles have been identified in tomato (Alexander and Grierson, 2002), but only a limited number of these compounds, such as hexanal, *trans*-2-hexanal, hexenol, *cis*-3-hexanol, 3-methylbutanal, 3-methylbutanol and methylnitrobutane, are the principal contributors to tomato flavor (Carrari and Fernie, 2006). These characteristic tomato aromas are formed by several different processes, i.e. lipid oxidation of polyunsaturated fatty acids (LOX pathway), deamination and decarboxylation of amino acids, and oxidative cleavage of carotenoids (Goff and Klee, 2006). Among these processes, the LOX pathway is the main process responsible for the production of aromas (Buttery *et al.*, 1987; Goff and Klee, 2006). At least three enzymes, i.e. LOX, HPL and ADH, are involved in the LOX pathway for aroma formation (Schwab *et al.*, 2008). LOX is an iron-containing dioxygenase that catalyzes the dioxygenation of polyunsaturated fatty acids (e.g. linoleic acid and linolenic acids) (Liavonchanka and Feussner, 2006), leading to generation of two possible products, the 9- and 13-hydroperoxide. The resulting hydroperoxides then serve as substrates for HPL to produce

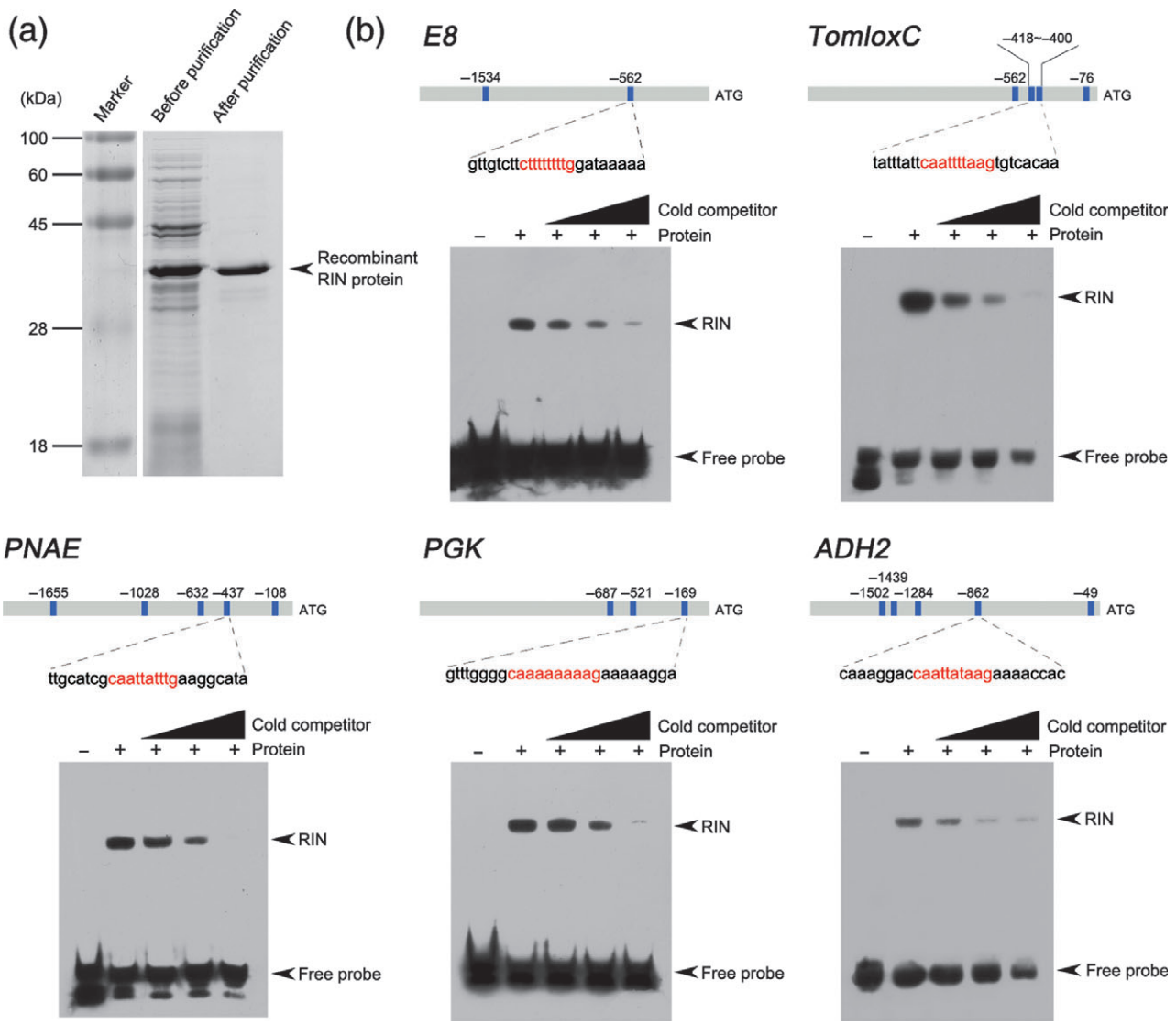

Figure 5. Electrophoretic mobility shift assay of RIN binding to the regulatory regions of target genes.
(a) SDS–PAGE gel stained with Coomassie blue demonstrating affinity purification of the recombinant RIN protein used for the electrophoretic mobility shift assay (EMSA).
(b) RIN binds directly to the promoters of downstream target genes containing CArG box elements. Blue boxes represent CArG box elements in the promoter region and numbers indicate the position of these motifs relative to the translational start site. The probe sequences corresponding to the promoters of each target genes are shown, with red letters representing the CArG box. The purified recombinant RIN protein was mixed with biotin-labeled probes, and the protein–DNA complexes were separated on 6% native polyacrylamide gels. Triangles indicate increasing amounts of unlabeled probes for competition.

aldehydes (hexanal and *cis*-3-hexenal). The primary HPL products are further converted by ADH into hexenol, *cis*-3-hexenol and others (Yilmaz *et al.*, 2001).

In the proteomic analysis, we detected down-regulation of LOX and ADH2 in the *rin* mutant. The changes in expression of LOX and ADH2 also occurred at the mRNA level, as revealed by quantitative RT-PCR. Tomato LOX is encoded by a family of at least five genes, *TomloxA–E*, of which *TomloxC* is responsible for the formation of aroma volatiles (Chen *et al.*, 2004). Two isoforms of ADH have been identified in tomato. ADH1 is present only in pollen, seeds and young seedlings, while ADH2 accumulates during fruit ripening concomitant with accumulation of flavor volatiles (Alexander and Grierson, 2002). Although *TomloxC* and *ADH2* are expressed upon fruit ripening, little is known about the regulatory mechanisms controlling expression of these two genes in the biosynthesis of aroma compounds. We examined the promoter regions of *TomloxC* and *ADH2* and found four and five CArG motifs, respectively (Table S2). To investigate whether *TomloxC* and *ADH2* are directly regulated by RIN, a ChIP assay was performed to probe DNA–protein interactions within the natural chromatin. Our results showed that RIN binds to the promoters of *TomloxC* and *ADH2 in vivo* (Figure 4b).

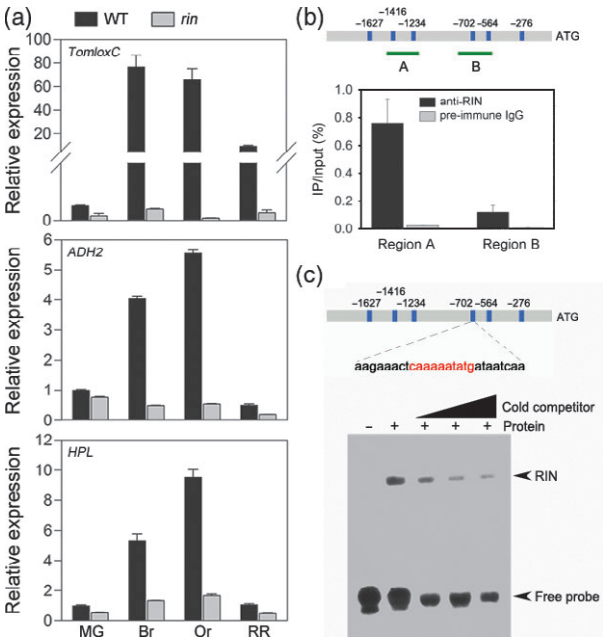

Figure 6. RIN directly regulates the expression of genes encoding enzymes in the lipoxygenase pathway.
(a) Gene expression analysis of *TomloxC*, *ADH2* and *HPL* in wild-type (WT) and *rin* mutant tomatoes during the period of fruit ripening, as determined by quantitative RT-PCR. The *18S rRNA* gene was used as the internal control. Values are means ± SD of three independent experiments. The stages of fruit ripening include mature green (MG), breaker (Br), orange (Or) and red ripe (RR).
(b) ChIP-qPCR assay for direct binding of RIN protein to the promoter of the *HPL* gene.
(c) *In vitro* binding analysis of RIN to the promoter of *HPL* containing CArG box elements. The symbols in (b) and (c) are the same as those described in Figures 4 and 5.

Further analysis using EMSA confirmed the results of ChIP analysis, showing that RIN bound to the promoters of *TomloxC* and *ADH2* (Figure 5b). In addition to *TomloxC* and *ADH2*, we examined RIN binding sites in the *HPL* promoter. Interestingly, six CArG box elements were found within the 2000 bp upstream region of the *HPL* promoter. The ChIP assay and the EMSA indicated that RIN protein had the ability to bind to the promoter of *HPL* (Figure 6b,c).

Detection of representative aroma compounds derived from the LOX pathway showed that the levels of aroma volatiles were markedly reduced in the mutant (Figure 7), concomitant with the decrease in gene expression. Taken together, these results suggest that the RIN transcription factor functions to directly regulate the LOX pathway at multiple points and to modulate aroma formation during tomato fruit ripening. Elucidation of the regulatory mechanism involved in this specific pathway has potential use in fruit quality improvement, in preference to targeting a single enzyme. Thus our study may be useful for future improvement of fruit flavor via genetic modifications.

RIN regulates the expression of genes required for ethylene synthesis

The plant hormone ethylene has been comprehensively investigated for regulation of fruit ripening. Biosynthesis of ethylene in plant tissues begins with methionine metabolism (Yang, 1985), in which *S*-adenosylmethionine synthetase catalyzes the conversion of methionine to *S*-adenosylmethionine. The *S*-adenosylmethionine is then converted to 1-aminocyclopropane-1-carboxylic acid (ACC) via ACC synthase, followed by subsequent metabolism of ACC to ethylene by 1-aminocyclopropane-1-carboxylate oxidase. In this process, the peptide methionine sulfoxide reductase E4 may be required for the methionine cycle. As a hormone that plays vital regulatory roles in fruit ripening, the biosynthesis of ethylene must be precisely regulated (Li *et al.*, 2011). RIN has been shown to directly regulate the expression of *ACS2* and *ACS4* by binding to their promoters during fruit ripening in tomato (Ito *et al.*, 2008; Fujisawa *et al.*, 2011). However, it remains unclear whether RIN directly regulates the expression of other genes involved in ethylene synthesis.

In the present study, we found that the *E8* promoter was directly bound by RIN in the ChIP assay and the EMSA (Figures 4b and 5b). E8, which shows 34% amino acid sequence identity with 1-aminocyclopropane-1-carboxylate oxidase (Deikman and Fischer, 1988), participates in feedback regulation of ethylene biosynthesis in the fruit ripening process (Kneissl and Deikman, 1996). Reduction in the levels of E8 protein by antisense suppression of the *E8* gene in tomato results in an increased level of ethylene production (Peñarrubia *et al.*, 1992), whereas induction of E8 production by over-expression of the gene leads to a corresponding reduction in ethylene synthesis (Kneissl and Deikman, 1996). *E8* is transcriptionally activated at the onset of fruit ripening (Lincoln and Fischer, 1988), but the regulatory mechanisms are not fully understood. It has been speculated that *E8* gene expression is controlled in fruit by RIN via activation of ethylene synthesis (Giovannoni, 2004). However, our results show that RIN directly regulates the transcriptional expression of *E8* by binding to its promoter.

A recent report by Martel *et al.* (2011) showed that the *E4* promoter was bound by RIN *in vivo*. There are three CArG box elements located at −48, −758, and −1667 relative to the translation start site in the promoter of the *E4* gene. The authors used a primer set flanking the CArG box at −48 for ChIP-qPCR, and observed significant enrichment of this promoter fragment (Martel *et al.*, 2011). In this study, we designed two primer sets flanking the CArG boxes at −48 and −758 in the *E4* promoter. However, the relative amounts of precipitated promoter fragments were very low, suggesting that RIN does not bind the promoter of the *E4* gene (data not shown). This discrepancy could be caused by the higher purity of our antibody which was affinity-purified using AminoLink Plus coupling resin.

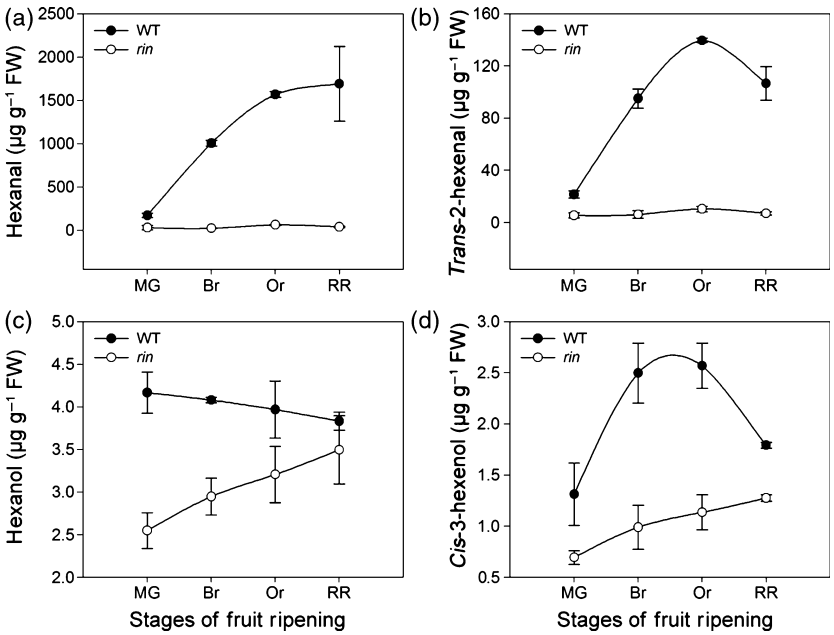

Figure 7. Production of volatile aroma compounds derived from the lipoxygenase pathway is regulated by RIN.
The levels of aroma compounds, including hexanal (a), *trans*-2-hexanal (b), hexenol (c) and *cis*-3-hexanol (d), were determined in wild-type (WT) and *rin* mutant tomato fruits. The stages of fruit ripening include mature green (MG), breaker (Br), orange (Or) and red ripe (RR). Similar results were obtained from three independent experiments, and a typical result with SD values is presented.

Regulation of carbohydrate-related genes by RIN

Another striking feature revealed by our proteomic analysis is the change in expression of proteins associated with carbohydrate metabolism in the *rin* mutant. Among the proteins identified, cytosolic fructose-1,6-bisphosphatase (cFBP) and TIV1 are involved in sucrose metabolism (Faurobert *et al.*, 2007). cFBP catalyzes the first irreversible reaction of the sucrose synthesis pathway, and is critical for photosynthetic carbon partition between sucrose and starch (Zrenner *et al.*, 1996). TIV1 catalyzes the hydrolysis of sucrose into glucose and fructose (Elliott *et al.*, 1993). Analysis of the promoter sequences of *TIV1* and *cFBP* showed that there was one CArG box binding motif in the promoter of each gene (Table S2). However, the ChIP assay indicated that RIN did not bind to the promoters of *TIV1* and *cFBP*. These results suggest that not all of the CArG box elements serve as binding sites for RIN, and that expression of *TIV1* and *cFBP* is indirectly regulated by RIN.

The cleavage products of sucrose can enter glycolysis and the tricarboxylic acid (TCA) cycle for production of ATP and NADH (Sturm, 1999). We identified two proteins, PGK and ICDH-1 (isocitrate dehydrogenase [$NADP^+$]), which are involved in glycolysis and the TCA cycle, respectively. Glycolysis and the TCA cycle are of central importance to the tomato fruit, but relatively little is currently known concerning their regulation (Carrari and Fernie, 2006). The results of the ChIP assay and the EMSA showed that RIN protein directly binds to the promoter of the *PGK* gene (Figures 4b and 5b). PGK catalyzes the transfer of a phosphate group from 1,3-bisphosphoglycerate to ADP, forming ATP and 3-phosphoglycerate. The ATP produced could provide the energy that is required during fruit ripening. Together, these results suggest that RIN regulates carbohydrate metabolism at multiple points directly or indirectly during tomato fruit ripening.

In summary, this work has led to the identification of downstream target genes of the transcription factor RIN. Expression analysis combined with ChIP assay and EMSA revealed that several crucial genes, i.e. *TomloxC*, *ADH2*, *HPL*, *E8*, *PNAE* and *PGK*, are directly regulated by RIN. These results suggest that RIN plays a fundamental role in the formation of characteristic volatile aroma compounds, and that it may also be fundamental in ethylene biosynthesis and carbohydrate metabolic processes. Our study provides new insights into understanding of the regulatory network of RIN in fruit ripening.

EXPERIMENTAL PROCEDURES

Plant material

Wild-type tomato (*Solanum lycopersicum* cv. Ailsa Craig) and a near-isogenic line carrying the *rin* mutation were kindly provided by Dr James J. Giovannoni (Boyce Thompson Institute for Plant Research, Cornell University, Ithaca, NY). Plants were grown in the greenhouse using standard culture practices, with regular additions of fertilizer and supplementary lighting when required. Flowers were tagged on the day of anthesis, and fruits were harvested at mature green (MG), breaker (Br), orange (Or) and red ripe (RR) stages, which occurred at means of 42, 44, 46 and 48 days post-anthesis (DPA), respectively. Ripening stages were confirmed on the basis of the size, shape, pigmentation, seed development and the development of locular jelly in the fruit as described previously (Alba *et al.*, 2005). Fruits of the *rin* mutant were picked at the equivalent ripening stages as determined by the number of DPA. Immediately upon harvesting, pericarp was manually dissected, frozen in liquid nitrogen, and stored at –80°C until use.

Two-dimensional (2D) gel electrophoresis of total protein extracts

For proteomic analysis, fruits were harvested at the breaker and orange ripening stages, and the total cellular proteins were extracted as described by Saravanan and Rose (2004). The proteins were solubilized in thiourea/urea lysis buffer consisting of 7 M urea, 2 M thiourea, 4% CHAPS, 1% dithiothreitol (DTT) and 2% carrier ampholytes, pH 4–7. Protein concentrations were determined by the Bradford method (1976) using bovine serum albumin as a standard. Aliquots of proteins (500 μg) were applied to rehydrate immobilized pH gradient gel strips (13 cm, pH 4–7 linear). Isoelectric focusing was performed using an Ettan IPGphor unit (GE Healthcare, http://www.gehealthcare.com) and the 2D electrophoresis was performed using 15% polyacrylamide gels (Qin *et al.*, 2009). After electrophoresis, proteins in the gel were visualized using Coomassie brilliant blue (CBB) R-250 (Sigma-Aldrich, http://www.sigmaaldrich.com/). The CBB-stained gels were scanned using a flatbed scanner (GE Healthcare), and stored in TIF format. Comparison of protein expression profiles between the wild-type and the *rin* mutant was performed using Image Master 2D Elite software (GE Healthcare).

In-gel digestion, mass spectrometry, and protein identification

Proteins in the gels were trypsin-digested before mass spectrometry. Tryptic peptides were analyzed on a Q-TOF micro mass spectrometer equipped with a CapLC HPLC system (Waters, http://www.waters.com/). MS and MS/MS spectra were acquired in automated data-dependent mode, and all data were processed using MassLynx version 4.0 software (Waters) to generate peak lists using the parameters smooth 3/2 Savitzky Golay and center 4 channels/80% centroid. The instrument was calibrated by multipoint calibration using selected fragment ions that resulted from collision-induced dissociation of Glu-fibrinopeptide B (+2 ion; *m/z* 785.8; Sigma-Aldrich, http://www.sigmaaldrich.com/).

For database searching, the generated peak lists were uploaded to the Mascot search program (http://www.matrixscience.com) using NCBInr protein databases (http://www.ncbi.nlm.nih.gov/protein). For proteins that had only one matching peptide or had multiple peptides for which each ion scored below the threshold, the Y-ion and B-ion series are presented in Figure S2. The matched peptides and individual peptide scores for the identified proteins are given in Table S4. Hierarchical clustering (Pearson's algorithm) was performed using PermutMatrix software version 1.9.3 (http://www.lirmm.fr/~caraux/PermutMatrix/index.html) (Caraux and Pinloche, 2005).

RNA isolation and quantitative RT-PCR analysis

RNA was isolated from the pericarp of at least 10 individual fruits using the method described by Moore *et al.* (2005). The extracted RNA was treated with DNase I (Promega, http://www.promega.com/) and first-strand cDNA was synthesized using M-MLV reverse transcriptase (Promega).

Quantitative real-time PCR was performed using an Mx3000P QPCR system (http://www.stratagene.com/) using SYBR Green PCR Master Mix (Applied Biosystems, http://www.appliedbiosystems.com/). Primer pairs (Table S5) for gene-specific quantitative RT-PCR of the selected genes were designed using Primer Express software 3.0 (Applied Biosystems). The PCR conditions were as follows: 95°C for 10 min, followed by 40 cycles of 95°C for 15 sec and 60°C for 30 sec. The change in fluorescence of SYBR Green in every cycle was monitored by the system software, and the threshold cycle (C_t) over the background was calculated for each reaction. Samples were normalized using *18S rRNA* (SGN accession number U581385) and the relative expression levels were measured using the $2^{(-\Delta C_t)}$ analysis method.

Recombinant protein expression and RIN-specific antibody preparation

The full-length *RIN* cDNA was amplified from tomato cDNA using the primers RIN-F (5′-CGGGATCCATGGGTAGAGGGAAAGTAG-3′) and RIN-R (5′-CCGCTCGAGTCAAAGCATCCATCCAGGTAC-3′). The fragment was digested using *Bam*HI and *Xho*I, and inserted into the same restriction sites of the pET30a vector (Merck, http://www.merck-group.com/) to produce pET30a-RIN. This construct allows in-frame fusion of the coding region of *RIN* to an N-terminal histidine tag. The plasmid was transformed into *Escherichia coli* BL21(DE3) competent cells. The expression of recombinant protein was induced by isopropyl-1-thio-β-D-galactopyranoside. Recombinant RIN protein was purified using Ni-NTA His-Bind® resin according to the manufacturer's instructions (Merck) and used for EMSA.

For specific antibody preparation, a truncated form of *RIN* lacking the conserved MADS box as described previously (Zhu *et al.*, 2007) was amplified from pET30a-RIN and sub-cloned into the pET-30a vector. The plasmid was transformed into *E. coli* BL21(DE3), and expression and purification of the recombinant protein were performed as described above. The recombinant protein was further purified by preparative gel electrophoresis and used to immunize rabbits at Beijing Protein Institute Co. Ltd (China). Polyclonal antibody was affinity-purified from antisera using AminoLink Plus coupling resin (Thermo Scientific, http://www.thermoscientific.com/) according to the manufacturer's instructions. The specificity of the RIN antibody was confirmed by Western blot analysis using *in vitro*-translated recombinant protein and nuclei extracts from wild-type and the *rin* mutant.

Nuclear extraction and Western blotting

The procedure for nuclear isolation from tomato fruits was modified from that described by Bowler *et al.* (2004). Nuclear proteins were extracted by sonication on ice in lysis buffer comprising 100 mM Tris/HCl pH 7.4, 1 mM EDTA, 10% glycerol, 75 mM NaCl, 0.05% SDS, 0.1% Triton X-100 and protease inhibitor cocktail (Sigma-Aldrich). The homogenates were centrifuged at 25 000 ***g*** for 30 min at 4°C, and the nuclear extracts in the supernatant were collected. SDS–PAGE and subsequent immunoblotting using affinity-purified rabbit polyclonal anti-RIN were performed as described previously (Qin *et al.*, 2009).

Chromatin immunoprecipitation (ChIP) and quantitative PCR analysis

ChIP assays were performed as described by Bowler *et al.* (2004) with minor modifications. The fruit tissue was submerged in 1% formaldehyde to cross-link genomic DNA and protein, and then submitted to nuclear isolation. The enriched nuclei were then sonicated to shear DNA to an mean size of 500–1000 bp. A small aliquot of sonicated chromatin was reversely cross-linked and used as the input DNA control. The sonicated chromatin suspension was centrifuged (10,000 x ***g*** for 10 min at 4°C), and the supernatant was diluted 10-fold in ChIP dilution buffer. The chromatin solution was pre-cleared using Protein A/agarose/salmon sperm DNA beads (Millipore, http://www.millipore.com/) for 1 h at 4°C. Immunoprecipitation of RIN cross-linked DNA was performed using affinity-purified polyclonal antibody for 12 h at 4°C with rotation. The reaction with pre-immune serum IgG or without antibody added was used as a mock/negative control. The DNA–protein–antibody complex was captured on Protein A/agarose beads by incubating

for 1 h at 4°C. The beads were pelleted for 2 min at 200 × ***g*** at 4°C and washed sequentially for 10 min at 4°C with low-salt wash buffer, high-salt wash buffer, lithium chloride wash buffer, and TE buffer, and the immunoprecipitated material was eluted by gently rotating for 15 min at 65°C. Cross-linking of immunoprecipitated DNA was reversed by incubation in 0.2 M NaCl at 65°C overnight. After proteinase K treatment, the immunoprecipitated DNA was purified and eluted. The amount of each precipitated DNA fragment was determined by real-time quantitative PCR using the same conditions as for quantitative RT-PCR. Primers used for quantitative PCR amplification are listed in Table S3. The presence of CArG box elements in the promoters of selected genes was analyzed using PLACE Web Signal Scan (http://www.dna.affrc.go.jp/PLACE/signalup.html).

Electrophoretic mobility shift assay (EMSA)

For the EMSA, recombinant His-tagged RIN protein was expressed in *E. coli* and purified using Ni-NTA His Bind Resin (Merck). The binding ability of RIN to specific DNA sequences was determined using a Lightshift chemiluminescent EMSA kit (Thermo Scientific). The 3′ biotin end-labeled double-stranded DNA probes were prepared by annealing complementary oligonucleotides. The sequences of the biotin-labeled probes used are shown in Table S6 and Figure 5(b). Protein–DNA complexes were separated on 6% native polyacrylamide gels, and the biotin-labeled probes were detected according to the instructions provided by the manufacturer of the EMSA kit.

Analysis of aroma volatiles

Tomato aroma volatiles were detected using a headspace solid-phase microextraction (HS-SPME) method as described by Zhang *et al.* (2010). Aroma volatiles were identified based on comparison of retention times with those of authentic standards (Alfa Aesat, http://www.alfa.com/). Quantitative determination of aroma compounds was performed using the peak of the internal standard as a reference value, and levels were calculated on the basis of a standard curve of authentic compounds. The experiment was repeated twice.

ACKNOWLEDGEMENTS

We thank Dr Zhuang Lu for her help in the MS/MS analysis and Professor Li Li from the Department of Plant Breeding and Genetics, Cornell University for her valuable suggestions and careful correction of the manuscript. This work was supported by the National Basic Research Program of China (973 Program, grant number 2011CB100604), the National Natural Science Foundation of China (grant number 31030051), and the CAS/SAFEA International Partnership Program for Creative Research Teams (grant number 20090491019).

SUPPORTING INFORMATION

Additional Supporting Information may be found in the online version of this article:

Figure S1. Functional categorization of the differentially expressed proteins identified in *rin* mutant tomato fruit.

Figure S2. Annotated spectra for proteins identified by a single peptide or multiple peptides for which each ion scored below the threshold.

Table S1. Identification of the differentially expressed proteins in the *rin* mutant tomato fruit using ESI-Q-TOF MS/MS

Table S2. Predicted RIN binding motifs within the 2000 bp upstream region starting from ATG of each candidate target gene

Table S3. Primers used in the ChIP-qPCR analysis

Table S4. Scores and matched peptides of the identified proteins based on tandem mass spectrometry

Table S5. Primers for quantitative RT-PCR analysis

Table S6. Sequences of the probes used in the EMSA

Please note: As a service to our authors and readers, this journal provides supporting information supplied by the authors. Such materials are peer-reviewed and may be re-organized for online delivery, but are not copy-edited or typeset. Technical support issues arising from supporting information (other than missing files) should be addressed to the authors.

REFERENCES

Alba, R., Payton, P., Fei, Z., McQuinn, R., Debbie, P., Martin, G.B., Tanksley, S.D. and Giovannoni, J.J. (2005) Transcriptome and selected metabolite analyses reveal multiple points of ethylene control during tomato fruit development. *Plant Cell*, **17**, 2954–2965.

Alexander, L. and Grierson, D. (2002) Ethylene biosynthesis and action in tomato: a model for climacteric fruit ripening. *J Exp Bot.* **53**, 2039–2055.

Azkargorta, M., Fullaondo, A., Laresgoiti, U., Aloria, K., Infante, A., Arizmendi, J.M. and Zubiaga, A.M. (2010) Differential proteomics analysis reveals a role for E2F2 in the regulation of the Ahr pathway in T lymphocytes. *Mol. Cell Proteomics*, **9**, 2184–2194.

Barry, C.S. and Giovannoni, J.J. (2006) Ripening in the tomato *Green-ripe* mutant is inhibited by ectopic expression of a protein that disrupts ethylene signaling. *Proc. Natl Acad. Sci. USA*, **103**, 7923–7928.

Bowler, C., Benvenuto, G., Laflamme, P., Molino, D., Probst, A.V., Tariq, M. and Paszkowski, J. (2004) Chromatin techniques for plant cells. *Plant J.* **39**, 776–789.

Bradford, M.M. (1976) A rapid and sensitive method for the quantitation of microgram quantities of protein utilizing the principle of protein–dye binding. *Anal. Biochem.* **72**, 248–254.

Buttery, R.G., Teranishi, R. and Ling, L.C. (1987) Fresh tomato aroma volatiles: a quantitative study. *J. Agric. Food. Chem.* **35**, 540–544.

Caraux, G. and Pinloche, S. (2005) PermutMatrix: a graphical environment to arrange gene expression profiles in optimal linear order. *Bioinformatics*, **21**, 1280–1281.

Carrari, F. and Fernie, A.R. (2006) Metabolic regulation underlying tomato fruit development. *J Exp Bot.* **57**, 1883–1897.

Chen, G.P., Hackett, R., Walker, D., Taylor, A., Lin, Z.F. and Grierson, D. (2004) Identification of a specific isoform of tomato lipoxygenase (TomloxC) involved in the generation of fatty acid-derived flavor compounds. *Plant Physiol.* **136**, 2641–2651.

Cravatt, B.F., Simon, G.M. and Yates, J.R. III (2007) The biological impact of mass-spectrometry-based proteomics. *Nature*, **450**, 991–1000.

Deikman, J. and Fischer, R.L. (1988) Interaction of a DNA binding factor with the 5′-flanking region of an ethylene-responsive fruit ripening gene from tomato. *EMBO J.* **7**, 3315–3320.

Dirinck, P., Schreyen, L. and Schamp, N. (1977) Aroma quality evaluation of tomatoes, apples and strawberries. *J. Agric. Food. Chem.* **25**, 759–762.

Elliott, K.J., Butler, W.O., Dickinson, C.D., Konno, Y., Vedvick, T.S., Fitzmaurice, L. and Mirkov, T.E. (1993) Isolation and characterization of fruit vacuolar invertase genes from two tomato species and temporal differences in mRNA levels during fruit ripening. *Plant Mol. Biol.* **21**, 515–524.

Faurobert, M., Mihr, C., Bertin, N., Pawlowski, T., Negroni, L., Sommerer, N. and Causse, M. (2007) Major proteome variations associated with cherry tomato pericarp development and ripening. *Plant Physiol.* **143**, 1327–1346.

Fujisawa, M., Nakano, T. and Ito, Y. (2011) Identification of potential target genes for the tomato fruit-ripening regulator RIN by chromatin immunoprecipitation. *BMC Plant Biol.* **11**, 26.

Giovannoni, J.J. (2004) Genetic regulation of fruit development and ripening. *Plant Cell*, **16**(Suppl.), S170–S180.

Giovannoni, J.J. (2007) Fruit ripening mutants yield insights into ripening control. *Curr. Opin. Plant Biol.* **10**, 283–289.

Goff, S.A. and Klee, H.J. (2006) Plant volatile compounds: sensory cues for health and nutritional value? *Science*, **311**, 815–819.

Hackett, R.M., Ho, C., Lin, Z., Foote, H.C.C., Fray, R.G. and Grierson, D. (2000) Antisense inhibition of the *Nr* gene restores normal ripening to the tomato *Never-ripe* mutant, consistent with the ethylene receptor inhibition model. *Plant Physiol.* **124**, 1079–1085.

Ito, Y., Kitagawa, M., Ihashi, N., Yabe, K., Kimbara, J., Yasuda, J., Ito, H., Inakuma, T., Hiroi, S. and Kasumi, T. (2008) DNA-binding specificity, transcriptional activation potential, and the *rin* mutation effect for the tomato fruit-ripening regulator RIN. *Plant J.* **55**, 212–223.

Karlova, R., Rosin, F.M., Busscher-Lange, J., Parapunova, V., Do, P.T., Fernie, A.R., Fraser, P.D., Baxter, C., Angenent, G.C. and de Maagd, R.A. (2011) Transcriptome and metabolite profiling show that APETALA2a is a major regulator of tomato fruit ripening. *Plant Cell*, **23**, 923–941.

Kevany, B.M., Tieman, D.M., Taylor, M.G., Cin, V.D. and Klee, H.J. (2007) Ethylene receptor degradation controls the timing of ripening in tomato fruit. *Plant J.* **51**, 458–467.

Kneissl, M.L. and Deikman, J. (1996) The tomato *E8* gene influences ethylene biosynthesis in fruit but not in flowers. *Plant Physiol.* **112**, 537–547.

Lelong, C., Rolland, M., Louwagie, M., Garin, J. and Geiselmann, J. (2007) Mutual regulation of Crl and Fur in *Escherichia coli* W3110. *Mol. Cell Proteomics*, **6**, 660–668.

Lewinsohn, E., Schalechet, F., Wilkinson, J. *et al.* (2001) Enhanced levels of the aroma and flavor compound S-linalool by metabolic engineering of the terpenoid pathway in tomato fruits. *Plant Physiol.* **127**, 1256–1265.

Li, L., Zhu, B., Yang, P., Fu, D., Zhu, Y. and Luo, Y. (2011) The regulation mode of RIN transcription factor involved in ethylene biosynthesis in tomato fruit. *J. Sci. Food Agric.* **91**, 1822–1828.

Liavonchanka, A. and Feussner, I. (2006) Lipoxygenases: occurrence, functions and catalysis. *J. Plant Physiol.* **163**, 348–357.

Lin, Z., Hong, Y., Yin, M., Li, C., Zhang, K. and Grierson, D. (2008) A tomato HD-Zip homeobox protein, LeHB-1, plays an important role in floral organogenesis and ripening. *Plant J.* **55**, 301–310.

Lin, Z., Zhong, S. and Grierson, D. (2009) Recent advances in ethylene research. *J Exp Bot.* **60**, 3311–3336.

Lincoln, J.E. and Fischer, R.L. (1988) Diverse mechanisms for the regulation of ethylene-inducible gene expression. *Mol. Gen. Genet.* **212**, 71–75.

Manning, K., Tor, M., Poole, M., Hong, Y., Thompson, A.J., King, G.J., Giovannoni, J.J. and Seymour, G.B. (2006) A naturally occurring epigenetic mutation in a gene encoding an SBP-box transcription factor inhibits tomato fruit ripening. *Nat. Genet.* **38**, 948–952.

Martel, C., Vrebalov, J., Tafelmeyer, P. and Giovannoni, J.J. (2011) The tomato MADS-box transcription factor RIPENING INHIBITOR interacts with promoters involved in numerous ripening processes in a COLORLESS NONRIPENING-dependent manner. *Plant Physiol.* **157**, 1568–1579.

Matas, A.J., Gapper, N.E., Chung, M.Y., Giovannoni, J.J. and Rose, J.K. (2009) Biology and genetic engineering of fruit maturation for enhanced quality and shelf-life. *Curr. Opin. Biotechnol.* **20**, 197–203.

Moore, S., Payton, P., Wright, M., Tanksley, S. and Giovannoni, J. (2005) Utilization of tomato microarrays for comparative gene expression analysis in the Solanaceae. *J Exp Bot.* **56**, 2885–2895.

Oeller, P.W., Lu, M.W., Taylor, L.P., Pike, D.A. and Theologis, A. (1991) Reversible inhibition of tomato fruit senescence by antisence RNA. *Science*, **254**, 437–439.

Peñarrubia, L., Aguilar, M., Margossian, L. and Fischer, R.L. (1992) An antisense gene stimulates ethylene hormone production during tomato fruit ripening. *Plant Cell*, **4**, 681–687.

Qin, G., Meng, X., Wang, Q. and Tian, S. (2009) Oxidative damage of mitochondrial proteins contributes to fruit senescence: a redox proteomics analysis. *J. Proteome Res.* **8**, 2449–2462.

Ruepp, A., Zollner, A., Maier, D. *et al.* (2004) The FunCat, a functional annotation scheme for systematic classification of proteins from whole genomes. *Nucleic Acids Res.* **32**, 5539–5545.

Saravanan, R.S. and Rose, J.K. (2004) A critical evaluation of sample extraction techniques for enhanced proteomic analysis of recalcitrant plant tissues. *Proteomics*, **4**, 2522–2532.

Schwab, W., Davidovich-Rikanati, R. and Lewinsohn, E. (2008) Biosynthesis of plant-derived flavor compounds. *Plant J.* **54**, 712–732.

Song, H., Kong, W., Weatherspoon, N., Qin, G., Tyler, W., Turk, J., Curtiss, R. III and Shi, Y. (2008) Modulation of the regulatory activity of bacterial two-component systems by SlyA. *J. Biol. Chem.* **283**, 28158–28168.

Sturm, A. (1999) Invertases: primary structures, functions, and roles in plant development and sucrose partitioning. *Plant Physiol.* **121**, 1–7.

Vrebalov, J., Ruezinsky, D., Padmanabhan, V., White, R., Medrano, D., Drake, R., Schuch, W. and Giovannoni, J. (2002) A MADS-box gene necessary for fruit ripening at the tomato *Ripening-inhibitor* (*Rin*) locus. *Science*, **296**, 343–346.

Vrebalov, J., Pan, I.L., Arroyo, A.J. *et al.* (2009) Fleshy fruit expansion and ripening are regulated by the tomato *SHATTERPROOF* gene *TAGL1*. *Plant Cell*, **21**, 3041–3062.

Yang, S.F. (1985) Biosynthesis and action of ethylene. *Hortic. Sci.* **20**, 41–45.

Yilmaz, E., Tandon, K.S., Scott, J.W., Baldwin, E.A. and Shewfelt, R.L. (2001) Absence of a clear relationship between lipid pathway enzymes and volatile compounds in fresh tomatoes. *J. Plant Physiol.* **158**, 1111–1116.

Zhang, B., Shen, J.Y., Wei, W.W., Xi, W.P., Xu, C.J., Ferguson, I. and Chen, K. (2010) Expression of genes associated with aroma formation derived from the fatty acid pathway during peach fruit ripening. *J. Agric. Food. Chem.* **58**, 6157–6165.

Zhu, H.L., Zhu, B.Z., Zhang, Y.L., Shao, Y., Wang, X.G., Xie, Y.H., Chen, A.J., Li, Y.C., Tian, H.Q. and Luo, Y.B. (2007) Expression of a truncated ripening inhibitor (RIN) protein from tomato and production of an anti-RIN antibody. *Biotechnol. Lett.* **29**, 1425–1430.

Zrenner, R., Krause, K.P., Apel, P. and Sonnewald, U. (1996) Reduction of the cytosolic fructose-1,6-bisphosphatase in transgenic potato plants limits photosynthetic sucrose biosynthesis with no impact on plant growth and tuber yield. *Plant J.* **9**, 671–681.

